Steady-state kinetics of the tungsten containing aldehyde Ferredoxin oxidoreductases from the hyperthermophilic archaeon Pyrococcus furiosus

Hagedoorn, P. L.

DOI
10.1016/j.jbiotec.2019.10.005

Publication date
2019

Document Version
Accepted author manuscript

Published in
Journal of Biotechnology

Citation (APA)
Hagedoorn, P. L. (2019). Steady-state kinetics of the tungsten containing aldehyde: Ferredoxin oxidoreductases from the hyperthermophilic archaeon Pyrococcus furiosus. *Journal of Biotechnology*, *306*, 142-148. https://doi.org/10.1016/j.jbiotec.2019.10.005

Steady-state kinetics of the tungsten containing aldehyde:ferredoxin oxidoreductases from the hyperthermophilic archaeon *Pyrococcus furiosus*

Peter-Leon Hagedoorn[‡,*]

[‡]Department of Biotechnology, Delft University of Technology, Van der Maasweg 9, 2629HZ, Delft, The Netherlands

*To whom correspondence should be addressed: Tel: +31-152782334

AUTHOR EMAIL: p.l.hagedoorn@tudelft.nl

KEYWORDS *Pyrococcus furiosus*; tungsten enzyme; glyceraldehyde-3-phosphate oxidoreductase; aldehyde ferredoxin oxidoreductase; steady state kinetics

The tungsten containing Aldehyde:ferredoxin oxidoreductases (AOR) offer interesting opportunities for biocatalytic approaches towards aldehyde oxidation and carboxylic acid reduction. The hyperthermophilic archaeon *Pyrococcus furiosus* encodes five different AOR family members: glyceraldehyde-3-phosphate oxidoreductase (GAPOR), aldehyde oxidoreductase (AOR), and formaldehyde oxidoreductase (FOR), WOR4 and WOR5. GAPOR functions as a glycolytic enzyme and is highly specific for the substrate glyceraldehyde-3-phosphate (GAP). AOR, FOR and WOR5 have a broad substrate spectrum, and for WOR4 no substrate has been identified to date. As ambiguous kinetic parameters have been reported for different AOR family enzymes the steady state kinetics under different physiologically relevant conditions was explored. The GAPOR substrate GAP was found to degrade at 60°C by non-enzymatic elimination of the phosphate group to methylglyoxal with a half-life $t_{1/2}$ = 6.5 min. Methylglyoxal is not a substrate or inhibitor of GAPOR. D-GAP was identified as the only substrate oxidized by GAPOR, and the kinetics of the enzyme was unaffected by the presence of L-GAP, which makes GAPOR the first enantioselective enzyme of the AOR family. The steady-state kinetics of GAPOR showed partial substrate inhibition, which assumes the GAP inhibited form of the enzyme retains some activity. This inhibition was found to be alleviated completely by a 1 M NaCl resulting in increased enzyme activity at high substrate concentrations. GAPOR activity was strongly pH dependent, with the optimum at pH 9. At pH 9, the substrate is a divalent anion and, therefore, positively charged amino acid residues are likely to be involved in the binding of the substrate. FOR exhibited a significant primary kinetic isotope effect of the apparent V_{max} for the deuterated

substrate, formaldehyde-d_2, which shows that the rate-determining step involves a C-H bond break from the aldehyde. The implications of these results for the reaction mechanism of tungsten-containing AORs, are discussed.

1. Introduction[1]

Pyrococcus furiosus is a hyperthermophilic archaeon that grows optimally at 100ºC, pH 7.0, and 0.5 M NaCl (Falia and Stetter, 1986). Five different members of the aldehyde: ferredoxin oxidoreductase family are encoded on the genome and all five have been isolated: aldehyde oxidoreductase (AOR), formaldehyde oxidoreductase (FOR), glyceraldehyde-3-phosphate oxidoreductase (GAPOR), WOR4 and WOR5. Each of these contains a mononuclear tungsten center bound to two pterin cofactors in their active site and a [4Fe-4S] cluster. The crystal structures of AOR and FOR, and sequence comparison with the known genomes, have shown that the aldehyde:ferredoxin oxidoreductase family of enzymes almost exclusively consists of tungsten enzymes (Roy et al., 1999). The only exception is (2R)-hydroxycarboxylate-viologen-oxidoreductase, which has been shown to be a molybdenum-containing enzyme (Trautwein et al., 1994).

[1] **Abbreviations**

AOR	Aldehyde oxidoreductase
BV	Benzyl viologen
EPR	Electron Paramagnetic Resonance
FOR	Formaldehyde oxidoreductase
GAP	Glyceraldehyde-3-phosphate
GAPOR	Glyceraldehyde-3-phosphate oxidoreductase
KIE	Kinetic isotope effect
MCD	Magnetic Circular Dichroïsm

It has been proposed that AOR and FOR oxidize aldehydes produced during amino acid breakdown; however, to date no physiological substrates have been identified for these enzymes. GAPOR is a key enzyme in the glycolysis of *P. furiosus*. For WOR4 no substrate has been identified to date (Roy and Adams, 2002). WOR5 has been shown to be an aldehyde oxidoreductase with a broad substrate specificity (Bevers et al., 2005). The nature and properties of the tungsten centers of AOR, FOR, WOR5 and GAPOR have been characterized by EPR and MCD spectroscopy (Arendsen et al., 1996; Bevers et al., 2005; Bol et al., 2006; Dhawan et al., 2000; Hagedoorn et al., 1999; Koehler et al., 1996). These studies have revealed that, in each of these enzymes, the tungsten center cycles between the oxidation states VI, V, and IV with midpoint potentials between *ca.* –600 and –400 mV.

Most characterized AOR family members are from hyperthermophilic archaea such as *P. furiosus*, *Pyrobaculum aerophilum* and *Thermococcus litoralis* (Hagedoorn et al., 2005; Mukund and Adams, 1993; Reher et al., 2007). However, a growing number of thermophilic and mesophilic bacterial AOR family members have been described from: *Moorella thermoacetica*, *Aromatoleum aromaticum*, *Geobacter metallireducens*, *Eubacterium acidaminophilum* (Arndt et al., 2019; Huber et al., 1994; Huwiler et al., 2019; Rauh et al., 2004; Strobl et al., 1992; White et al., 1991). The AOR family member from *Geobacter metallireducens*, BamB, is part of a large complex redox enzyme involved in benzene dearomatization (Huwiler et al., 2019). Recently, a novel AOR family member was identified in the thermophilic bacterium *Caldicellulosiruptor bescii*, which was shown to be a new heterodimeric type of GAPOR (Scott et al., 2015; Scott et al., 2019). *C. bescii* was found to serve as a host for the functional heterologous expression of *P. furiosus* AOR. Recombinant expression of GAPOR from a mesophilic methanogenic archaeon *Methanococcus maripaludis*

in *E. coli* resulted in a functional Mo containing enzyme (Park et al., 2007). *E. coli* contains an AOR homolog on its genome YdhV, which very recently has been recombinantly produced and characterized for the first time (Reschke et al., 2019).

Although some information on the steady state kinetics of these tungsten enzymes has been obtained (Bol et al., 2008; Heider et al., 1995; Mukund and Adams, 1991, 1995; Roy et al., 1999)**,** we have much to learn about the structure-function relationship for these enzymes. Herein, we present more information concerning the steady-state kinetics of the GAPOR that reveal aspects of the substrate inhibition of this enzyme. Here, the steady state kinetics of different AOR family enzymes under different physiologically relevant conditions was further explored. GAPOR was found to be specific for D-GAP, which is the first example of enantioselectivity in the AOR family. The dependence of the activity of GAPOR on pH and temperature was investigated and compared to the corresponding aspects of AOR. Furthermore, kinetic isotope effect (KIE) for formaldehyde oxidation by FOR using deuterated formaldehyde was determined, which revealed a C-H bond break is involved in the rate determining step of the catalytic mechanism.

2. MATERIALS AND METHODS

2.1 Cultivation and enzyme purification

Pyrococcus fusiosus (DSM 3638) was cultivated in a 200 liter fermentor at 90°C, as described previously (Arendsen et al., 1995). Aldehyde oxidoreductase (AOR), formaldehyde oxidoreductase (FOR), glyceraldehyde-3-phosphate oxidoreductase (GAPOR) were purified under anaerobic conditions as described elsewhere (Mukund and Adams, 1991, 1993, 1995).

2.2 Glyceraldehyde-3-phosphate stability

The degradation of glyceraldehyde-3-phosphate (GAP) at 60°C in 100 mM potassium phosphate buffer, pH 7.0, was studied by analyzing samples, drawn every minute, for aldehyde content using the Purpald method (Dickinson and Jacobsen, 1970) - a colorimetric procedure that employs 3-hydrazino-5-mercapto-1,2,4-triazole (Purpald, as obtained from Sigma-Aldrich). To 800 µl water, 100 µl aldehyde sample, 100 µl 50 mg/ml purpald in 1 M NaOH and 4 µl 30% H_2O_2 was added. The UV-vis spectrum was recorded after 2 hour color development.

2.3 Substrate inhibition of GAPOR

GAPOR activity was assayed anaerobically in 50 mM EPPS/tricine buffer pH (25°C) 8.4 containing 8 µM deazaflavin using benzyl viologen (BV) reduction, monitoring the optical absorbance at 580 nm (ε_{580} = 7,800 $M^{-1}cm^{-1}$) (Mukund and Adams, 1995). The benzyl viologen in the cuvette was pre-reduced to a light blue color using light exposure and deazaflavin/tricine to ensure anaerobic conditions. Activity measurements with D,L-GAP concentrations of: 0.005, 0.01, 0.02, 0.03, 0.05, 0.1, 0.2, 0.5, 1.0 mM were measured in the presence of 1, 3, or 5 mM BV.

The data were analyzed using a model that assumed partial uncompetitive substrate inhibition of the enzyme, see equation **1** (Wang et al., 1999).

$$V_0 = \frac{V_{max}[S](1+b\frac{[S]}{K_i})}{K_M+[S](1+\frac{[S]}{K_i})} \qquad \text{Eq. } \mathbf{1}$$

The parameter *b* is the ratio between the v at infinite substrate concentration and apparent V_{max} and, hence, represents the extent of the inhibition. If $b = 0$, the regular description of Michaelis-Menten kinetics with complete substrate inhibition is obtained; if $K_I \rightarrow \infty$, equation **1** becomes the regular, uninhibited, Michaelis-Menten equation.

2.4 Enantioselectivity towards D- and L-GAP

GAPOR activity was assayed anaerobically as described above, using 3 mM BV with D,L-GAP and D-GAP as substrates. The D-GAP content of commercially available D,L-GAP (Sigma) was measured enzymatically using rabbit muscle GAPDH (Furfine and Velick, 1965). D-GAP was produced from D-glyceraldehyde-3-phosphate diethyl acetal (Sigma-Aldrich) using Dowex 50W 4x200 (Supelco) as previously described (Furfine and Velick, 1965). The concentration D-GAP was determined enzymatically using GAPDH. The GAP oxidation was determined form the BV_{red} concentration using a molar extinction coefficient for the BV_{red} ε_{600nm} = 11.6 mM^{-1} cm^{-1} and correcting for the fact that GAP is 2 electron oxidized, and BV is one electron reduced.

2.5 Effect of sodium chloride, pH and temperature on GAPOR activity

GAPOR activity was assayed anaerobically at 60°C as described above, using 3 mM BV with 0.5 mM D,L-GAP as substrates. The activity was measured in: 50 mM MES pH 5.3 and 6.0;

MOPS pH 6.9; EPPS/tricine pH 7.8; EPPS pH 7.9; CHES pH 8.3, 8.5, 8.8, 9.2, and 9.4; and CAPS pH 9.7 and 10.5 – these pH values are for 60°C. The GAPOR activity with EPPS/tricine pH_{60} 7.8 was measured between 20 and 80°C. At temperatures above 80°C the GAPOR activity measurements were practically not possible due to instability of the substrate. To investigate the effect of the sodium chloride, the GAPOR activity was measured at 60°C, using 3 mM BV in 50 mM EPPS/tricine pH_{60} 7.8 with 0.5 mM D,L-GAP in the presence of 0, 0.1, 0.2, or 1 M NaCl.

AOR activity was assayed anaerobically from 25- 98°C in 50 mM EPPS/tricine buffer pH (25°C) 8.4 containing 8 μM deazaflavin and using 1 mM BV and 0.3 mM crotonaldehyde as substrates. The pH dependence of AOR activity was measured at 60°C using 50 mM MES pH 6.4; EPPS pH 7.5; CHES pH 8.3, 8.6, 9.6; and CAPS pH 10.3 and 11.1 – these pH values are for 60°C.

2.6 Deuterium kinetic isotope effect (KIE) on FOR activity

The deuterium KIE of the substrate at 70ºC was measured for FOR in a non-deuterated assay buffer using formaldehyde or formaldehyde-d_2 (20% solution in D_2O, Aldrich) as the substrate. FOR activity was measured anaerobically in 50 mM EPPS/tricine buffer pH (25°C) 8.4 containing 1 mM methyl viologen and 50 μM deazaflavin. The methyl viologen in the cuvettes were pre-reduced by exposure to light using deazflavin/tricine to a light blue color. The free formaldehyde concentration was 0.4% of the total formaldehyde concentration at 70°C (Winkelman et al., 2002).

3 RESULTS

3.1 Glyceraldehyde 3-phosphate stability

Although GAP is relatively stable in its free acid form, the dianion, which is the major species at ambient and basic pH, it is highly sensitive towards non-enzymatic elimination of the phosphate group. This non-enzymatic reaction is likely to be more pronounced at high temperatures and, therefore, is of relevance to the *in vitro* activity assays of GAPOR and the metabolism of GAP in *Pyrococcus furiosus*. Possible breakdown or isomerization products of GAP are: glyceraldehyde, dihydroxyacetone phosphate, and methylglyoxal (Humeres and Quijano, 1996). By using the Purpald assay to measure the aldehyde substrate and product concentrations we have found that GAP, when incubated at 60°C and pH 7, is hydrolyzed to methylglyoxal (Fig. 1a and Scheme 1); this degradation follows first order kinetics with $k = 0.103 \pm 0.006$ min^{-1} for GAP disappearance and $k = 0.11 \pm 0.01$ min^{-1} for methylglyoxal appearance at 60ºC (Fig. 1b). The half-life of GAP at 60°C was $t_{1/2} = 6.5$ min.

Methylglyoxal gives a very characteristic adduct in the Purpald assay with a maximal absorbance at 384 nm, unlike the normal aldehyde adduct which has an absorbance at 525 nm. This is a consequence of the α-keto-group, which changes the electron delocalization of the Purpald adduct chromophore (supplementary Fig. S1). The time trace of the GAP degradation shows a clear isosbestic point at 444 nm, which indicates that there are no other aldehyde products or intermediates in the degradation process. Glyceraldehyde and dihydroxyacetone phosphate have been shown not to be substrates or inhibitors of GAPOR (Mukund and Adams, 1995), however, the interaction of methylglyoxal with this enzyme has never been reported. Furthermore, commercially available D,L-GAP has been reported to contain 3-15%

methylglyoxal (McLellan et al., 1992). Therefore, the effects of this compound on GAPOR are relevant to kinetic measurements accomplished using commercially available D,L-GAP. We have found that methylglyoxal was not a substrate for GAPOR, and GAPOR activity with GAP as a substrate was unaffected by 5.5 mM methylglyoxal (not shown).

3.2 Substrate inhibition of GAPOR

As reported previously (Mukund and Adams, 1995), GAPOR is significantly inhibited by GAP at > 0.5 mM, however, the apparent K_m and V_{max} values were determined without taking this substrate inhibition into account. Substrate inhibition may cause large differences between the apparent K_m and V_{max} values, based only on data from measurements at low substrate concentrations, and the real K_m and V_{max} values. Inhibition of GAPOR by GAP was most prominent at low BV concentration (see supplemental Fig. S2). The activity dependent on the substrate concentration did not follow regular Michaelis-Menten kinetics (at each electron acceptor concentration). The deviation from regular Michaelis-Menten kinetic could be due to substrate inhibition since the substrate concentration was the only parameter that was varied during the kinetic trace. However, the activity profiles did not approach zero at high substrate concentrations, which you would expect for regular (uncompetitive) substrate inhibition. The activity appeared to stabilize at higher substrate concentrations, after an initial higher activity at lower substrate concentrations, which points towards partial substrate inhibition. Therefore, the kinetic data were interpreted by assuming partial substrate inhibition of the enzyme: *i.e.* the substrate-inhibited form of the enzyme retained some activity. Consistently the K_i for GAP was at least 10 times smaller than the K_M. This suggests that GAPOR has a high affinity inhibitory binding site for GAP.

3.3 GAPOR is enantioselective and only converts D-GAP

The conversion of D-GAP and the racemic mixture D,L-GAP by GAPOR, as measured by the reduction of BV at 60°C resulted in *ca.* 100% of D-GAP and *ca.* 50% of D,L-GAP oxidized respectively (supplementary Fig. S3a and b). D-GAP is the only substrate of GAPOR and L-GAP is not oxidized (or is oxidized at a much lower rate than D-GAP). The activity profiles of GAPOR with D-GAP and D,L-GAP are depicted in supplementary Fig. S3c. These profiles match when the activity is plotted against the D-GAP concentration. Again, this is consistent with D-GAP being the only substrate of GAPOR and it appears that L-GAP is not an inhibitor of GAPOR when present in equimolar quantities with D-GAP.

3.4 Effect of sodium chloride, pH and temperature on GAPOR activity

The pH dependence of GAPOR activity can be described by assuming two pK_a values, each of *ca.* 9 (see Fig. 2b). This pH dependence differs from that for AOR (Fig. 2a), for which no pK_a values can be determined. The pK_a values of GAP at 50°C have been reported: (i) from free acid to monoanion, $pK_a = 1.60$; (ii) from monoanion to dianion, $pK_a = 6.66$ (scheme 1 and (Humeres and Quijano, 1996)). Therefore, it appears that is the substrate for GAPOR is D-GAP dianion.

The temperature dependence of AOR activity (Fig. 2c) fits excellent to the Eyring equation up to 80°C, involving a single free energy of activation $\Delta G^{\ddagger} = 74.01 \pm 0.03$ kJ·mol^{-1}. No additional fit-parameters were required, and the fit was also excellent in the lower temperature range from 25-40°C (inset of Fig. 2c). This confirms a previous reported value of 75 kJ·mol^{-1} for the activation energy for *Thermococcus* ES-1 AOR (Heider et al., 1995). The temperature

dependence of GAPOR (Fig. 2d) did not fit to the Eyring equation but rather showed an almost linear increase of the k_{cat} with temperature. This shows that multiple temperature dependent effects are in play, and markedly different than AOR. It is important to note that the substrate GAP is unstable at high temperatures.

Fig. 3 shows the effect of NaCl on the activity of GAPOR. Clearly, the activity of GAPOR is strongly dependent on the NaCl concentration, however, this dependence was less pronounced at lower GAP concentrations. The activity profiles show that the effect of partial substrate inhibition is reduced as the NaCl concentration increases and, for a concentration [NaCl] = 1 M, the GAPOR activity profile fits to regular Michaelis-Menten kinetics. A global fit of the four traces of Fig. 3, assuming partial substrate inhibition and common apparent V_{max} and b values, resulted in values of apparent K_m and K_I that were dependent on the sodium chloride concentration; thus, high a NaCl concentration decreases the affinity of GAP towards both its substrate (higher K_m) and inhibitory binding site (higher K_i).

3.6 Substrate kinetic isotope effect of FOR

The substrate KIE of FOR (Fig. 4) is ${}^{D}V_{max,\ apparent}$ = 3.0 ± 0.4, at pH 8.4 and 70°C, and represents a significant primary isotope effect for C-H bond breaking at this temperature (Melander and Saunders, 1980). Furthermore, there was no KIE of the K_m. This is strong evidence that C-H bond break of formaldehyde is the rate-determining step in the catalytic mechanism of FOR.

4 DISCUSSION

4.1 Glyceraldehyde 3-phosphate thermal degradation to methylglyoxal

The degradation of GAP at high temperatures (>50°C) has not been investigated previously. Methylglyoxal was found to be the major product of the non-enzymatic degradation under assay conditions of GAPOR. This is a consequence of a base catalyzed mechanism that starts with the abstraction of a proton at C2, leading to an enediol intermediate with subsequent leaving of the phosphate group (Humeres and Quijano, 1996). Methylglyoxal does not interfere with GAPOR activity, however, it may have physiological consequences for *P. furiosus,* since it is toxic for most organisms (Kalapos, 1999). There is no evidence yet for *in vivo* production of methylglyoxal by *P. furiosus*. However, we note that the boiling point of methylglyoxal is 70°C, which is also the minimum growth temperature of *P. furiosus* (Stetter, 1999). Oxidation of methyglyoxal to pyruvate by any of the AOR family enzymes has not been reported.

4.2 Steady state kinetics of GAPOR

We have found GAPOR to be subject to partial substrate inhibition by GAP. This inhibition may be a mode of regulation for this glycolytic enzyme. GAPOR is monomeric, and therefore conventional allosteric control is not possible (Mukund and Adams, 1995). The nature of the inhibition by this substrate is not known, but it is likely that GAPOR has a separate inhibitory binding site for GAP. The pH and temperature dependence of GAPOR was determined at the relatively high substrate concentration of 0.5 mM GAP since substrate inhibition does not allow measurement under apparent V_{max} conditions. Although the enzyme is partially inhibited at this

267 substrate concentration, the adopted procedure was convenient since the activity of GAPOR is
268 relatively independent of substrate concentration in the range 0.3-0.6 mM GAP (Fig. 3 and S2).
269 GAPOR has a narrow substrate specificity and, in only D-GAP was oxidized with a significant
270 rate by GAPOR. This is a property that this enzyme has in common with glyceraldehyde-3-
271 phosphate dehydrogenase (GAPDH). GAPOR was apparently not inhibited by L-GAP;
272 therefore, a racemic mixture of D-GAP and L-GAP can be used for kinetic measurements. These
273 results have not been confirmed using only L-GAP as a substrate for GAPOR.
274 The activity of the enzyme was strongly pH dependent with an optimal activity occurring at pH
275 9. At this pH the substrate is exclusively present as the dianion, which suggests that positively
276 charged groups (*e.g.* Lys or Arg) are necessary for substrate binding. Clearly, the negatively
277 charged phosphate group is important for recognition of the substrate, since GAPOR shows no
278 activity towards glyceraldehyde or methylglyoxal. Furthermore, the dependence of GAPOR
279 activity on the sodium chloride concentration of the solution reflects the influence of charged
280 groups on the binding of the substrate and the release of the product.
281 GAPOR activity did not follow the Eyring equation, which may be a consequence of the
282 thermal instability of the substrate GAP. It is important to note that these enzymes are thus active
283 at room temperature. The physiological temperature of *P. furiosus* is *ca.* 100°C and, as discussed
284 above, at this temperature the substrate GAP is unstable. Therefore, a mechanism to protect the
285 substrate would appear to be necessary, to allow glycolysis to function effectively at this
286 temperature; however, the nature of this mechanism is not known.
287 Ambiguous kinetic parameters have been previously reported for GAPOR: the apparent V_{max} in
288 the BV reduction assay for this enzyme range from 25 U/mg (van der Oost et al., 1998) to 350

U/mg (Mukund and Adams, 1995). This large difference in the apparent V_{max} cannot be fully explained by the different assay temperatures of 50°C and 70°C, respectively (Fig. 2d), however, it can be explained by the differences in the BV concentration (1 and 3 mM) and the GAP concentration (1.5 and 0.4 mM), as can be seen in Fig. 3 and supplementary Fig. S2. The results of the kinetic study presented here can be used to predict GAPOR activity under a wide range of conditions.

Although substrate inhibition has been suggested previously, it was not included in the determination of the reported values of the apparent V_{max} and K_m (Mukund and Adams, 1995). Substrate inhibition has also been reported for *M. maripaludis* GAPOR heterologously expressed in *E. coli* (Park et al., 2007). Also, it has been reported, without explanation, that GAPOR activity is stimulated by the presence of potassium phosphate, sodium arsenate, potassium chloride, sodium citrate, or sodium sulfate (Mukund and Adams, 1995). Here we show that GAPOR activity is strongly affected by sodium chloride. High salt concentrations may reduce the affinity of GAP for the inhibitory binding site of GAPOR, thereby alleviating the partial substrate inhibition which results in higher activities at high concentrations of GAP. High sodium chloride concentration affects not only the affinity of GAP to the inhibitory binding site, but also to the substrate binding site, as was manifested by the higher apparent K_m value at 1 M NaCl. The results of the global fitting of all steady-state kinetic data at different NaCl concentrations showed that the apparent V_{max} of GAPOR for D-GAP is much higher than previously reported, i.e. 470 U/mg at 60°C and this high initial rate can be achieved at 1 M NaCl and > 1 mM DL-GAP.

4.3 Evidence for a rate determining C-H bond break in the catalytic mechanism of FOR

FOR was found to exhibit a significant primary deuterium KIE for the oxidation of formaldehyde-d_2. Therefore, it appears that the breaking of the aldehyde C-H bond is a rate-determining step in the catalysis by the W-containing AORs. Although the crystal structures of AOR and FOR are ambiguous in respect of the oxo- or hydroxo- coordination of the tungsten, a mechanism has been proposed involving nucleophilic attack by a tungsten-bound water molecule on the α-carbon of the aldehyde, followed by hydride transfer to the oxo-ligand of the tungsten has been suggested (Chan et al., 1995; Hu et al., 1999). A computational study by Himo and co-workers suggested that formaldehyde binds to the W^{IV} center of FOR directly, followed by a nucleophilic attach of the W=O oxo group to the substrate carbonyl carbon atom forming a tetrahedral intermediate. A proton is abstracted from the intermediate substrate by Glu308 in concert with the 2 electron reduction of the W center, which was predicted to be the rate determining step (Liao et al., 2011). This is consistent with the observed $^{D}V_{max,\ apparent}$ for FOR.

ACKNOWLEDGMENT

This research has been financially supported by the Council for Chemical Sciences of the Netherlands Organization for Scientific Research (CW-NWO). The authors would like to thank Juul Slits and Dr. J. Robert Freije for the isolation of GAPOR. Prof. Wilfred R. Hagen is acknowledged for valuable discussions.

REFERENCES

Arendsen, A.F., De Vocht, M., Bulsink, Y.B.M., Hagen, W.R., (1996) Redox Chemistry of Biological Tungsten: An EPR Study of the Aldehyde Oxidoreductase from *Pyrococcus furiosus*. J. Biol. Inorg. Chem. 1, 292-296.

Arendsen, A.F., Veenhuizen, P.T.M., Hagen, W.R., (1995) Redox Properties of the Sulfhydrogenase from *Pyrococcus furiosus*. FEBS Lett. 368, 117-121.

Arndt, F., Schmitt, G., Winiarska, A., Saft, M., Seubert, A., Kahnt, J., Heider, J., (2019) Characterization of an Aldehyde Oxidoreductase From the Mesophilic Bacterium *Aromatoleum aromaticum* EbN1, a Member of a New Subfamily of Tungsten-Containing Enzymes. Front. Microbiol. 10.

Bevers, L.E., Bol, E., Hagedoorn, P.L., Hagen, W.R., (2005) WOR5: A Novel Tungsten Containing Aldehyde Oxidoreductase from *Pyrococcus furiosus* with a Broad Substrate Specificity. J. Bacteriol. 187, 7056-7061.

Bol, E., Bevers, L.E., Hagedoorn, P.L., Hagen, W.R., (2006) Redox Chemistry of Tungsten and Iron-Sulfur Prosthetic Groups in *Pyrococcus furiosus* Formaldehyde Ferredoxin Oxidoreductase. J. Biol. Inorg. Chem. 11, 999-1006.

Bol, E., Broers, N.J., Hagen, W.R., (2008) A steady-state and pre-steady-state kinetics study of the tungstoenzyme formaldehyde ferredoxin oxidoreductase from *Pyrococcus furiosus*. J. Biol. Inorg. Chem. 13, 75-84.

Chan, M.K., Mukund, S., Kletzin, A., Adams, M.W.W., Rees, D.C., (1995) Structure of a Hyperthermophilic Tungstopterin Enzyme, Aldehyde Ferredoxin Oxidoreductase. Science 267, 1463-1469.

Dhawan, I.K., Roy, R., Koehler, B.P., Mukund, S., Adams, M.W.W., Johnson, M.K., (2000) Spectroscopic Studies of the Tungsten-containing Formaldehyde Ferredoxin Oxidoreductase from the Hyperthermophilic Archaeon *Thermococcus litoralis*. J. Biol. Inorg. Chem. 5, 313-327.

Dickinson, R.G., Jacobsen, N.W., (1970) A New Sensitive and Specific Test for the Detection of Aldehydes: Formation of 6-Mercapto-3-Substituted-s-Triazolo[4,3-b]-s-Tetrazines. J. Chem. Soc. D, 1719-1720.

Falia, G., Stetter, K.O., (1986) *Pyrococcus furiosus* sp. nov. represents a Novel Genus of Marine Heterotrophic Archaeabacteria growing Optimally at 100°C. Arch. Microbiol. 145, 56-61.

Furfine, C.S., Velick, S.F., (1965) The Acyl-Enzyme Intermediate and the Kinetic Mechanism of the Glyceraldehyde 3-Phosphate Dehydrogenase Reaction. J. Biol. Chem. 240, 844-855.

Hagedoorn, P.L., Chen, T., Schröder, I., Piersma, S.R., De Vries, S., Hagen, W.R., (2005) Purification and characterization of the tungsten enzyme aldehyde:ferredoxin oxidoreductase from the hyperthermophilic denitrifier *Pyrobaculum aerophilum*. J. Biol. Inorg. Chem. 10, 259-269.

Hagedoorn, P.L., Freije, J.R., Hagen, W.R., (1999) *Pyrococcus furiosus* Glyceraldehyde 3-phosphate Oxidoreductase has Comparable W(6+/5+) and W(5+/4+) Reduction Potentials and Unusual [4Fe-4S] EPR Properties. FEBS Lett. 462, 66-70.

Heider, J., Ma, K., Adams, M.W., (1995) Purification, characterization, and metabolic function of tungsten-containing aldehyde ferredoxin oxidoreductase from the hyperthermophilic and proteolytic archaeon Thermococcus strain ES-1. J. Bacteriol. 177, 4757-4764.

Hu, Y., Faham, S., Roy, R., Adams, M.W.W., Rees, D.C., (1999) Formaldehyde Ferredoxin Oxidoreductase from *Pyrococcus furiosus*: The 1.85 Å Resolution Crystal Structure and its Mechanistic Implications. J. Mol. Biol. 286, 899-914.

Huber, C., Caldeira, J., Jongejan, J.A., Simon, H., (1994) Further Characterization of Two Different, Reversible Aldehyde Oxidoreductases from *Clostridium formicoacteticum*, one Containing Tungsten and the Other Molybdenum. Arch. Microbiol. 162, 303-309.
Humeres, E., Quijano, J., (1996) The Mechanisms of Hydrolysis of Glyceraldehyde-3-phosphate. Gazz. Chim. Ital. 126, 449-456.
Huwiler, S.G., Löffler, C., Anselmann, S.E.L., Stärk, H.-J., von Bergen, M., Flechsler, J., Rachel, R., Boll, M., (2019) One-megadalton metalloenzyme complex in *Geobacter metallireducens* involved in benzene ring reduction beyond the biological redox window. Proc. Natl. Acad. Sci. USA 116, 2259-2264.
Kalapos, M.P., (1999) Methylglyoxal in Living Organisms. Chemistry, Biochemistry, Toxicology and Biological Implications. Toxicol. Lett. 110, 145-175.
Koehler, B.P., Mukund, S., Conover, R.C., Dhawan, I.K., Roy, R., Adams, M.W.W., Johnson, M.K., (1996) Spectroscopic Characterization of the Tungsten and Iron Centers in Aldehyde Ferredoxin Oxidoreductases from Two Hyperthermophilic Archaea. J. Am. Chem. Soc 118, 12391-12405.
Liao, R.-Z., Yu, J.-G., Himo, F., (2011) Tungsten-dependent formaldehyde ferredoxin oxidoreductase: Reaction mechanism from quantum chemical calculations. J. Inorg. Biochem. 105, 927-936.
McLellan, A.C., Phillips, S.A., Thornally, P.J., (1992) The Assay of Methylglyoxal in Biological Systems by Derivatization with 1,2-Diamino-4,5-dimethoxybenzene. Anal. Biochem. 206, 17-23.
Melander, L., Saunders, W.H., (1980) Reaction Rates of Isotopic Molecules. John Wiley & Sons, New York.
Mukund, S., Adams, M.W.W., (1991) The Novel Tungsten-Iron-Sulfur Protein of the Hyperthermophilic Archaebacterium, *Pyrococcus furiosus*, is an Aldehyde Ferredoxin Oxidoreductase. J. Biol. Chem. 266, 14208-14216.
Mukund, S., Adams, M.W.W., (1993) Characterization of a Novel Tungsten-containing Formaldehyde Ferredoxin Oxidoreductase from the Hyperthermophilic Archaeon, *Thermococcus litoralis*. J. Biol. Chem. 268, 13592-13600.
Mukund, S., Adams, M.W.W., (1995) Glyceraldehyde-3-phosphate Ferredoxin Oxidoreductase, a Novel Tungsten-containing Enzyme with a Potential Glycolytic Role in the Hyperthermophilic Archaeon *Pyrococcus furiosus*. J. Biol. Chem. 270, 8389-8392.
Park, M.O., Mizutani, T., Jones, P.R., (2007) Glyceraldehyde-3-phosphate ferredoxin oxidoreductase from *Methanococcus maripaludis*. J. Bacteriol. 189, 7281-7289.
Rauh, D., Graentzdoerffer, A., Granderath, K., Andreesen, J.R., Pich, A., (2004) Tungsten-containing aldehyde oxidoreductase of Eubacterium acidaminophilum. Eur. J. Biochem. 271, 212-219.
Reher, M., Gebhard, S., Schönheit, P., (2007) Glyceraldehyde-3-phosphate ferredoxin oxidoreductase (GAPOR) and nonphosphorylating glyceraldehyde-3-phosphate dehydrogenase (GAPN), key enzymes of the respective modified Embden–Meyerhof pathways in the hyperthermophilic crenarchaeota *Pyrobaculum aerophilum* and *Aeropyrum pernix*. FEMS Microbiol. Lett. 273, 196-205.
Reschke, S., Duffus, B.R., Schrapers, P., Mebs, S., Teutloff, C., Dau, H., Haumann, M., Leimkühler, S., (2019) Identification of YdhV as the First Molybdoenzyme Binding a Bis-Mo-MPT Cofactor in *Escherichia coli*. Biochemistry 58, 2228-2242.

Roy, R., Adams, M.W.W., (2002) Characterization of a Fourth Tungsten-Containing Enzyme from the Hyperthermophilic Archaeon *Pyrococcus furiosus*. J. Bacteriol. 184, 6952-6956.
Roy, R., Mukund, S., Shut, G.J., Dunn, D.M., Weiss, R., Adams, M.W.W., (1999) Purification and Molecular Characterization of the Tungsten-Containing Formaldehyde Ferredoxin Oxidoreductase from the Hyperthermophilic Archaeon *Pyrococcus furiosus*: the Third of a Putative Five-Member Tungstoenzyme Family. J. Bacteriol. 181, 1171-1180.
Scott, I.M., Rubinstein, G.M., Lipscomb, G.L., Basen, M., Schut, G.J., Rhaesa, A.M., Lancaster, W.A., Poole, F.L., Kelly, R.M., Adams, M.W.W., (2015) A New Class of Tungsten-Containing Oxidoreductase in *Caldicellulosiruptor*, a Genus of Plant Biomass-Degrading Thermophilic Bacteria. Appl. Environ. Microbiol. 81, 7339-7347.
Scott, I.M., Rubinstein, G.M., Poole, F.L., Lipscomb, G.L., Schut, G.J., Williams-Rhaesa, A.M., Stevenson, D.M., Amador-Noguez, D., Kelly, R.M., Adams, M.W.W., (2019) The thermophilic biomass-degrading bacterium *Caldicellulosiruptor bescii* utilizes two enzymes to oxidize glyceraldehyde 3-phosphate during glycolysis. J. Biol. Chem. 294, 9995-10005.
Stetter, K.O., (1999) Extremophiles and their Adaptation to Hot Environments. FEBS Lett. 452, 22-25.
Strobl, G., Feicht, R., White, H., Lottspeich, F., Simon, H., (1992) The Tungsten-Containing Aldehyde Oxidoreductase from *Clostridium thermoaceticum* and its Complex with a Viologen-Accepting NADPH Oxidoreductase. Biol. Chem. 373, 123-132.
Trautwein, T., Krauss, F., Lottspeich, F., Simon, H., (1994) The (2R)-Hydroxycarboxylate-Viologen-Oxidoreductase from *Proteus vulgaris* is a Molybdenum-Containing Iron-Sulphur Protein. Eur. J. Biochem. 222, 1025-1032.
van der Oost, J., Schut, G.J., Kengen, S.W.M., Hagen, W.R., Thomm, M., de Vos, W.M., (1998) The Ferredoxin-dependent Conversion of Glyceraldehyde-3-phosphate in the Hyperthermophilic Archaeon *Pyrococcus furiosus* Represents a Novel Site of Glycolytic Regulation. J. Biol. Chem. 273, 28149-28154.
Wang, J., Araki, T., Ogawa, T., Matsouka, M., Fukuda, H., (1999) A Method of Graphically Analyzing Substrate-Inhibition Kinetics. Biotechnol. Bioeng. 62, 402-411.
White, H., Feicht, R., Huber, C., Lottspeich, F., Simon, H., (1991) Purification and Some Properties of the Tungsten-Containing Carboxylic Acid Reductase from *Clostridium formicoaceticum*. Biol. Chem. 372, 999-1005.
Winkelman, J.G.M., Voorwinde, O.K., Ottens, M., Beenackers, A.A.C.M., Janssen, L.P.B.M., (2002) Kinetics and chemical equilibrium of the hydration of formaldehyde. Chem. Eng. Sci. 57, 4067-4076.

455 **Scheme 1.** Fate of D-glyceraldehyde-3-phosphate under enzymatic assay conditions.

456

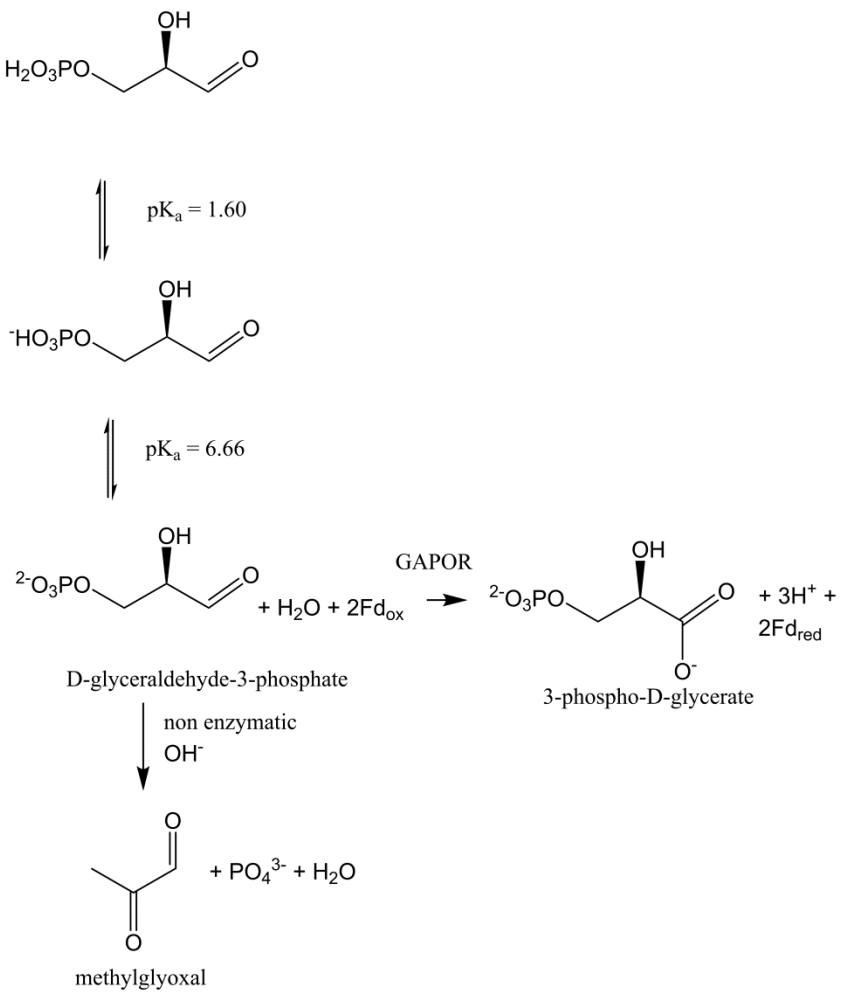

Legend to the figures

Fig. 1. GAP degradation at 60°C. (a) Optical absorption of the purpald product during incubation of GAP after 0, 1, 2, 3, 4, 5, 10, 20, 40, 60 minutes incubation at 60°C and pH 7.0. (b) First-order kinetics of the disappearance of glyceraldehyde-3-phosphate (■) and appearance of methylglyoxal (●) at 60°C and pH 7.0. The absorbance difference A384-A444 represented methylglyoxal and A525-A444 represented GAP. The data was fitted to a single exponential curve: $y = y_0 + y_{max}e^{-k \cdot t}$

Fig. 2. The pH dependent activities of (a) AOR and (b) GAPOR and the temperature dependent activities of (c) AOR and (d) GAPOR. The pH dependence of the AOR activity fitted to a line with the following equation: V_0 = -22 + 4.6·pH. The pH dependence of GAPOR activity fitted to the Henderson-Hasselbalch equation assuming two ionizable groups: $V_0 = \frac{V_{max,pH}}{1+\frac{10^{-pK_{a2}}}{10^{-pH}}+\frac{10^{-pH}}{10^{-pK_{a1}}}}$ with a $V_{max,pH}$ = 768 U/mg, $pK_{a,2}$ = 8.3, $pK_{a,1}$ = 9.6. The temperature dependence of AOR was fitted to the Eyring equation: $k_{cat} = \frac{k_B T}{h} e^{-\frac{\Delta G^{\ddagger}}{RT}}$ with Boltzmann constant k_B, planck constant h, Gas constant R, and $\Delta G^{\ddagger}$ as the only fit parameter. $\Delta G^{\ddagger}$ = 74.01 ± 0.03 kJ·mol^{-1} was obtained.

Fig. 3. Effect of sodium chloride on *P.furiosus* GAPOR activity. Sodium chloride concentrations of 0 (○), 0.1 (■), 0.2 (△) and 1 M (u). The solid lines represent fits to equation **1** assuming and

identical V_{max} and b values for all four traces (global fit). The fit parameters were: V_{max}, 470 ± 30 U/mg; b = 0.067 ± 0.014; K_M, 131 ± 36, 228 ± 33, 197 ± 23, 317 ± 42 μM; K_I, 5.0 ± 2.8, 57 ± 12, 114 ± 18 μM; for 0, 0.1, 0.2 and 1 M NaCl respectively. The K_I was not applicable for the 1M NaCl condition as it fitted to the regular Michaelis-Menten equation.

Figure 4. Kinetic isotope effect of *P.furiosus* FOR. FOR activity with formaldehyde (●) and formaldehyde-d_2 (●). The solid lines represent a global fit to the regular Michaelis-Menten equation in which the $K_{M,\ apparent}$ was set equal for both curves, resulting in the following fit parameters: $V_{max,\ apparent}$ = 4.1 ± 0.6 U/mg, $K_{M,\ apparent}$ = 0.22 ± 0.05 mM for formaldehyde and $V_{max,\ apparent}$ = 1.3 ± 0.2 U/mg, $K_{M,\ apparent}$ = 0.22 ± 0.05 mM formaldehyde-d_2. The resulting KIE $^{D}V_{max,\ apparent}$ = 3.0 ± 0.4.

488 Figure 1.

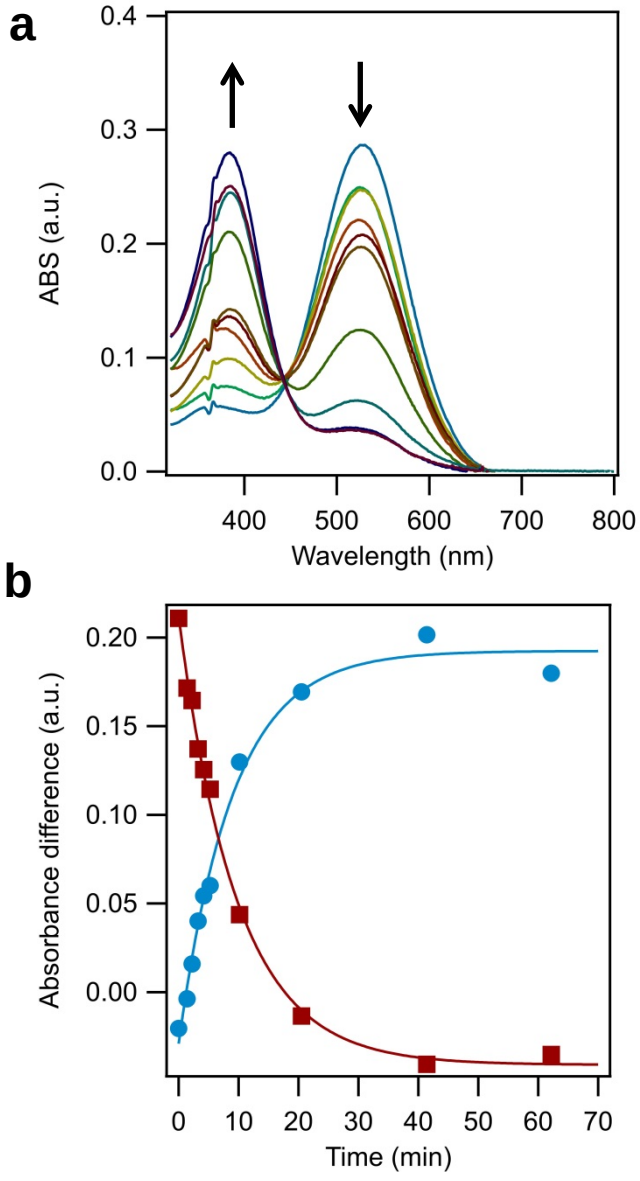
a
0.4
0.3
0.2
0.1
0.0
ABS (a.u.)
400
500
600
700
800
Wavelength (nm)
b
0.20
0.15
0.10
0.05
0.00
Absorbance difference (a.u.)
0
10
20
30
40
50
60
70
Time (min)

489 Figure 2.

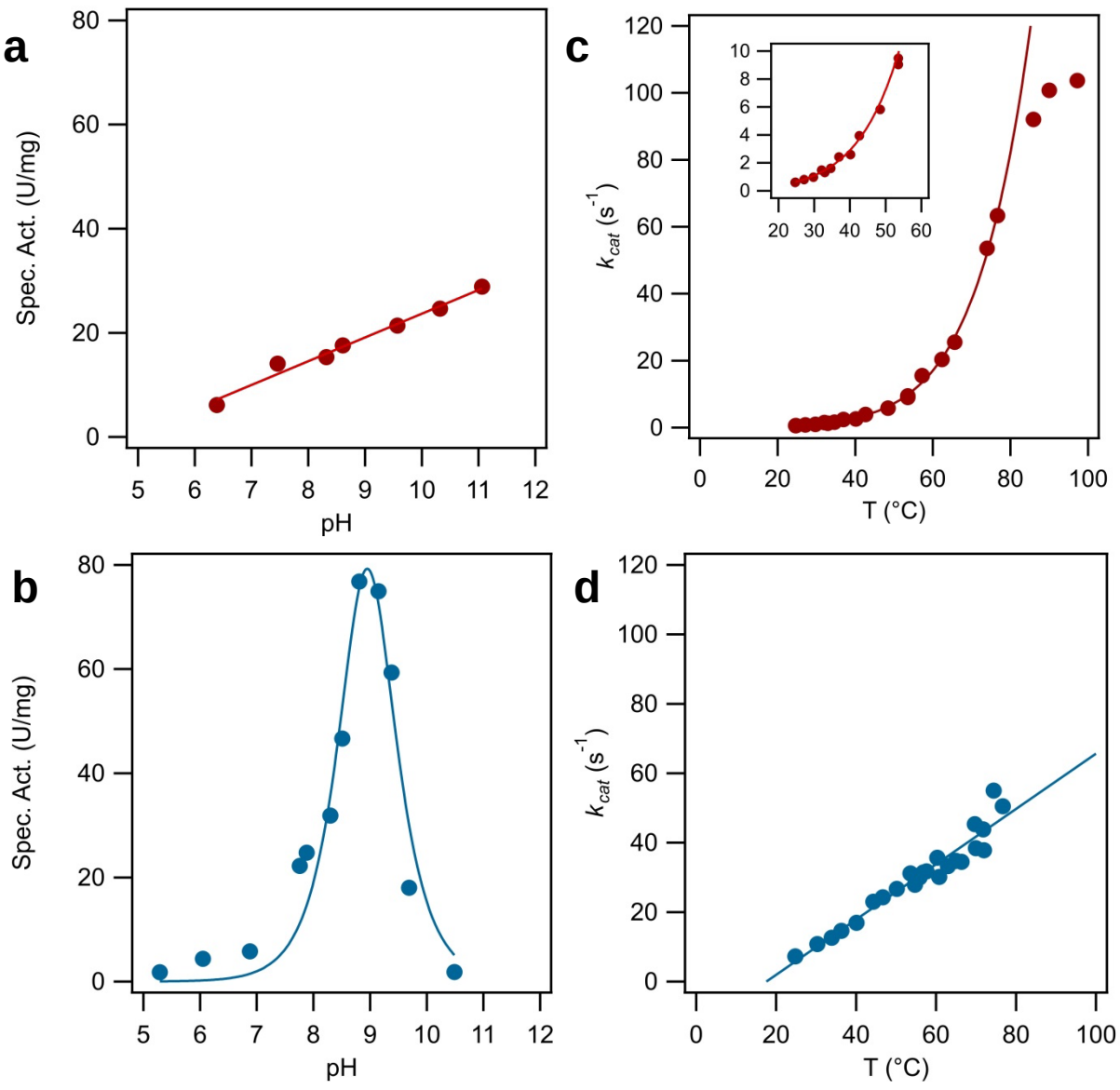

490 Figure 3.

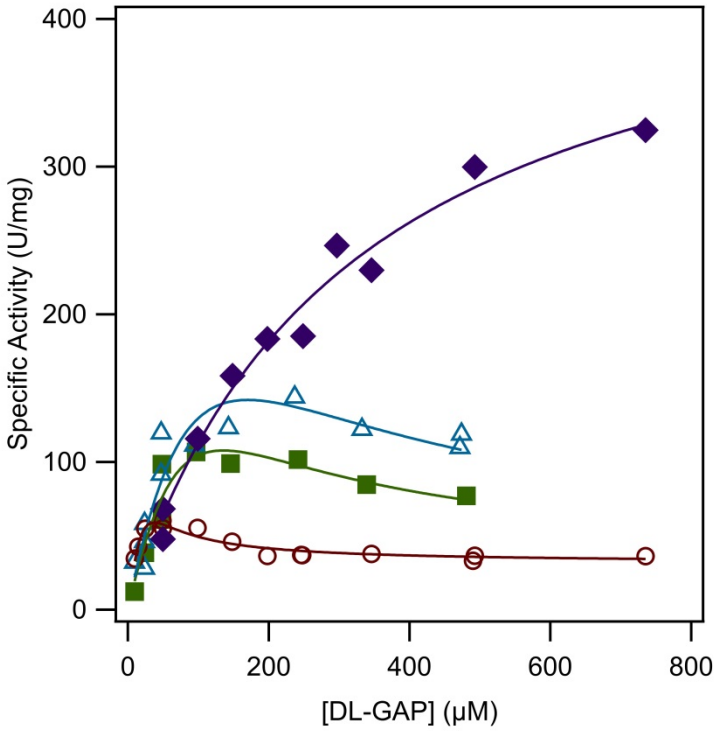
400
300
200
100
0
Specific Activity (U/mg)
0
200
400
600
800
[DL-GAP] (μM)

491 Figure 4.

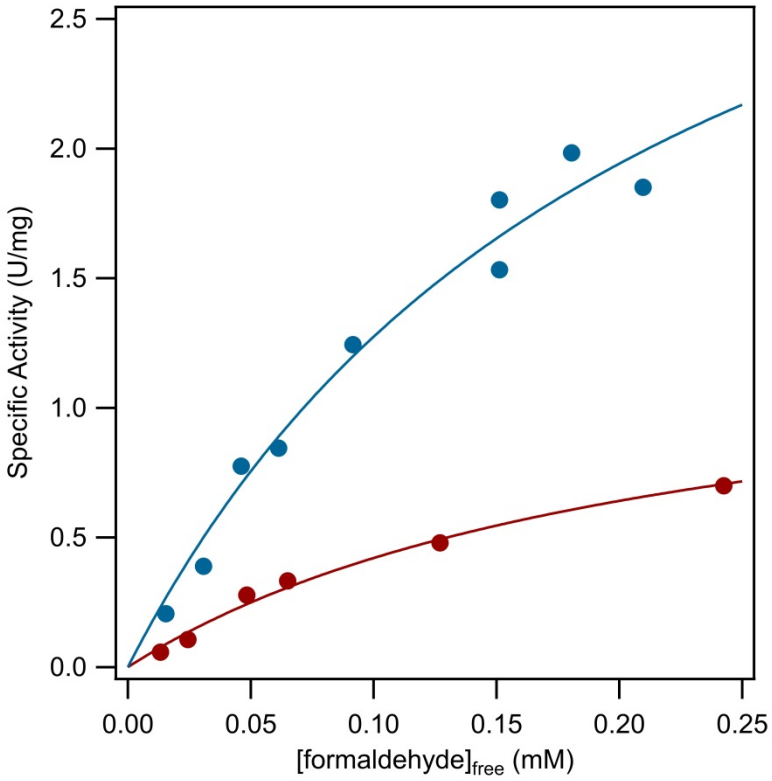
2.5
2.0
1.5
1.0
0.5
0.0
Specific Activity (U/mg)
0.00
0.05
0.10
0.15
0.20
0.25
[formaldehyde]free (mM)